RECENT ELECTROWEAK MEASUREMENTS WITH ATLAS*

Brigitte Vachon

on behalf of the ATLAS Collaboration

McGill University, Montréal, Canada

Received 15 April 2025, accepted 30 April 2025, published online 26 June 2025

The ATLAS experiment at the Large Hadron Collider continues to deliver high-precision measurements that probe the electroweak sector of the Standard Model. This summary highlights recent results using proton–proton collision data, including precision determinations of the W-boson mass and width, measurements of exclusive hadronic W decays, and studies of W- and Z-boson production. New insights into the electroweak gauge structure through studies of diboson polarization, radiation amplitude zero effects, and rare quartic gauge couplings are also reviewed. These results offer stringent tests of the Standard Model and increase sensitivity to potential New Physics.

DOI:10.5506/APhysPolBSupp.18.5-A34

1. Introduction

The electroweak sector of the Standard Model presents a rich phenomenology rooted in a non-Abelian gauge theory with spontaneous symmetry breaking. This framework leads to precise predictions for the properties and interactions of the gauge bosons.

The Large Hadron Collider (LHC) provides an unparalleled opportunity to test these predictions at high energies and with increasing precision. The ATLAS experiment [1] has made significant advances in both precision measurements and the study of rare electroweak processes. These results enable detailed investigations of electroweak symmetry breaking, gauge boson dynamics, and quantum loop effects, while also offering sensitivity to possible physics beyond the Standard Model.

* Presented at the 31st Cracow Epiphany Conference on the *Recent LHC Results*, Kraków, Poland, 13–17 January, 2025.

This paper presents a selection of recent ATLAS results, organized into two main categories: precision measurements of Standard Model parameters and studies probing the structure of the electroweak gauge sector. Together, these measurements test the internal consistency of the Standard Model and explore potential signs of new phenomena.

2. Measurement of Standard Model parameters

2.1. W-boson mass and width

A re-analysis of ATLAS data collected in 2011 has led to a high-precision measurement of the W-boson mass (m_W) and width (Γ_W) [2]. The motivation for these measurements was to consolidate earlier ATLAS results, particularly in light of the most recent CDF measurement [3] in tension with other W-boson mass measurements [4–7]. The updated ATLAS analysis benefits from improved statistical methods and updated parton distribution functions, enabling a more robust extraction of m_W and Γ_W.

The ATLAS results are based on fits to the reconstructed transverse W mass and lepton p_{T} distributions in $W \to \ell\nu$ decays. As demonstrated in Ref. [2], the sensitivity of these observables is such that a 0.1% change in m_W or a 10% change in Γ_W results in sub-percent level variations in the distributions. Consequently, stringent control over systematic uncertainties — particularly those related to lepton energy calibration and recoil modelling — was critical to achieving the reported precision.

The measured W-boson mass and width, obtained from two independent fits to the data, are

$$\begin{aligned} m_W &= 80.3665 \pm 0.0159 \text{ GeV}, \\ \Gamma_W &= 2.202 \pm 0.047 \text{ GeV}. \end{aligned}$$

The total uncertainty on m_W is reduced by approximately 15% compared to the previous ATLAS result based on the same dataset [6]. The W-boson width is determined with a precision of about 2%, representing the most precise single-experiment measurement to date and the first of its kind at the LHC. A simultaneous extraction of m_W and Γ_W is also performed, yielding the 68% and 95% confidence level contours shown in Fig. 1, with a correlation coefficient of -30% .

2.2. W + jet production

The large production cross section for single W bosons produced in association with jets enables detailed studies of kinematic observables in the high-momentum regime. A precise theoretical description of this process is essential, as it constitutes a significant irreducible background to many analyses across the LHC physics program.

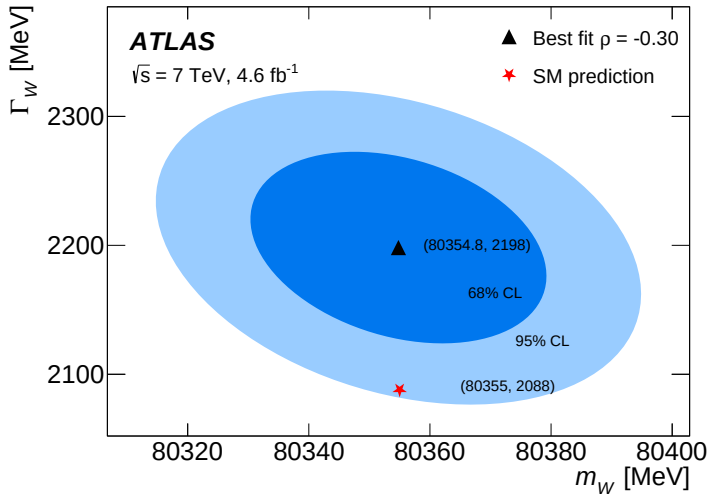

Fig. 1. Plot of the 68% and 95% confidence level uncertainty contours for the simultaneous determination of the W-boson mass (m_W) and width (Γ_W) obtained using the CT18 proton distribution functions, and by combining results from a fit to the lepton transverse momentum and reconstructed transverse mass distributions. The triangular marker represents the best fit, while the star corresponds to the Standard Model (SM) prediction [2].

To evaluate the accuracy of current state-of-the-art theoretical models, ATLAS has measured inclusive and differential cross sections in both the collinear and high transverse momentum regimes [8]. Multijet-merged next-to-leading-order (NLO) predictions from Sherpa and MadGraph provide good agreement with the data across the entire phase space explored. In contrast, fixed-order $W + 1$ jet calculations from MCFM at next-to-next-to-leading order (NNLO) offer small theoretical uncertainties comparable to the experimental precision, but fail to adequately describe regions of phase space where the W boson and leading jet are separated by a large angle.

2.3. W, Z, and ZZ production

The ATLAS Collaboration has recently published measurements of the total and differential production cross sections of W [9], Z [9], and ZZ [10] final states at the centre-of-mass energy of 13.6 TeV. These results constitute the first step in the programme of boson production studies at the new centre-of-mass energy of 13.6 TeV.

The total production cross sections of single W and Z bosons are measured with uncertainties at the 2–3% level, dominated by the uncertainty on the integrated luminosity. In contrast, the total ZZ production cross section is measured with a precision of approximately 6%, with statistical and systematic uncertainties contributing comparably.

Figure 2 summarizes these and other ATLAS measurements of total production cross sections across a range of processes and centre-of-mass energies. All results are consistent with Standard Model predictions.

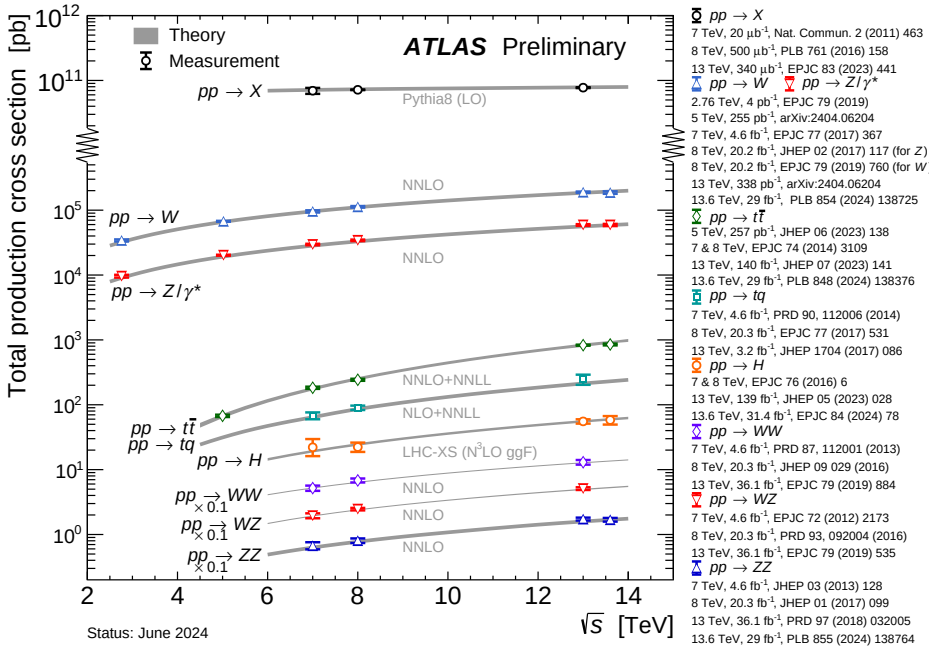

Fig. 2. Summary of total production cross-section measurements from ATLAS for selected processes, shown as a function of centre-of-mass energy from 2.76 to 13.6 TeV [11].

2.4. Exclusive W-boson hadronic decays

In addition to studying boson production, ATLAS also investigates their decays. A recent analysis reports the first limits on rare exclusive hadronic decays of the W boson involving a charged meson and a photon in the final state [12]. These decays are predicted in the Standard Model to have branching fractions of the order of 10^{-9}.

Such rare processes offer a unique opportunity to probe both the weakly- and strongly-coupled regimes of quantum chromodynamics (QCD) within a single decay. Moreover, they could provide a novel avenue for measuring

the W-boson mass through fully reconstructed final states at future colliders — potentially overcoming current limitations in precision from measurements relying on leptonic W decays.

A key innovation enabling this search is the use of a dedicated track-photon trigger signature. Results of this search are summarized in Table 1. This analysis achieves a factor of four improvement in sensitivity to the $W^{\pm} \to \pi^{\pm}\gamma$ decay as compared to previous published results [13], and sets the first upper limits on the branching fractions $\mathcal{B}(W^{\pm} \to K^{\pm}\gamma)$ and $\mathcal{B}(W^{\pm} \to \rho^{\pm}\gamma)$.

Table 1. Expected and observed upper limits on the $W^{\pm} \to \pi^{\pm}\gamma$, $W^{\pm} \to K^{\pm}\gamma$, and $W^{\pm} \to \rho^{\pm}\gamma$ branching fractions [12].

	95% confidence level upper limits	
Branching fraction	Expected $\times 10^{-6}$	Observed $\times 10^{-6}$
$\mathcal{B}(W^{\pm} \to \pi^{\pm}\gamma)$	$1.2^{+0.5}_{-0.3}$	1.9
$\mathcal{B}(W^{\pm} \to K^{\pm}\gamma)$	$1.1^{+0.4}_{-0.3}$	1.7
$\mathcal{B}(W^{\pm} \to \rho^{\pm}\gamma)$	$6.0^{+2.3}_{-1.7}$	5.2

2.5. Z-boson invisible decay width

The invisible decay width of the Z boson offers a fascinating window into potential New Physics. The ATLAS Collaboration measured the Z invisible width using a recoil-based technique that consists in measuring the ratio of $Z(\to \text{inv}) + \text{jets}$ to $Z(\to \ell\ell) + \text{jets}$ cross sections (R^{miss}) as a function of the Z transverse momentum [14]. Using this ratio measurement, the Z-boson invisible width is determined by utilising the measured value of the leptonic decay width, $\Gamma(Z \to \ell\ell)$, as

$$\Gamma(Z \to \text{inv}) = R^{\text{miss}}\, \Gamma(Z \to \ell\ell)\,. \tag{1}$$

The resulting measurement of the Z-boson invisible width is 506 $\pm$ 2(stat.) $\pm$ 12(syst.) MeV [14]. With a total uncertainty of approximately 2.5%, this measurement is the single most precise recoil-based measurement made to date. This result is consistent with the LEP Z lineshape measurement [15] and Standard Model expectations, demonstrating the ATLAS experiment ability to precisely test electroweak predictions.

3. Studies of the electroweak gauge structure

3.1. WZ polarization and radiation-amplitude zero

The study of diboson polarization provides a powerful probe of the gauge symmetry structure and the mechanism of electroweak symmetry breaking. Longitudinal polarization components arise from the Goldstone bosons associated with electroweak symmetry breaking, and gauge symmetry ensures the unitarity of longitudinal vector boson scattering cross sections at high energies.

With the increased dataset at the LHC, experiments are gaining sensitivity to the production of longitudinally polarized bosons ($V_{\mathrm{L}}V_{\mathrm{L}}$) and are starting to probe their energy dependence.

New results from ATLAS focus on the polarization states of WZ diboson production, specifically the longitudinally polarized $W_{\mathrm{L}}Z_{\mathrm{L}}$ contributions [16]. By selecting events with low jet activity and high transverse momentum of the Z boson (p_{T}^{Z}), the analysis enhances sensitivity to $W_{\mathrm{L}}Z_{\mathrm{L}}$ scattering. Using a boosted decision tree, evidence for $W_{\mathrm{L}}Z_{\mathrm{L}}$ production is found at high-Z transverse momentum ($p_{\mathrm{T}}^{Z} > 200$ GeV), with a statistical significance of 3.2σ.

A unique feature of the electroweak theory is the phenomenon of radiation-amplitude-zero, which arises from specific cancellations in some diboson scattering amplitudes at leading order.

The ATLAS Collaboration observed and studied this effect in transversely polarized WZ events by examining rapidity differences sensitive to interference effects [16]. The dependence of this effect on the transverse momentum of the WZ system is found to be in agreement with Standard Model expectations.

3.2. Quartic electroweak couplings

The form and strength of quartic gauge couplings in the Standard Model are fully determined by the underlying symmetry of the theory. Therefore, any observed deviations in the production cross section of processes directly sensitive to these couplings would provide an unambiguous signature of New Physics.

Processes primarily involving quartic gauge couplings are some of the rarest phenomena currently accessible at the LHC. These include diboson production via vector boson scattering and triboson production processes.

The ATLAS Collaboration observed the rare vector boson scattering processes $W\gamma jj$ [17] and $WZjj$ [18], mediated by electroweak diagrams, using advanced multivariate and machine learning techniques. The measured fidu-

cial cross sections for these processes are shown in Fig. 3 and are in good agreement with Standard Model expectations. These studies also feature detailed analyses of the modelling of key observables for both processes.

The ATLAS experiment is now also sensitive to triboson production. The ATLAS Collaboration reported the first observation of the $W\gamma\gamma$ production with a statistical significance of 5.6σ [19]. Additionally, a new analysis has achieved a 6σ observation for the production of three massive bosons where at least one is a Z boson, and a 4σ evidence of WWZ production [20].

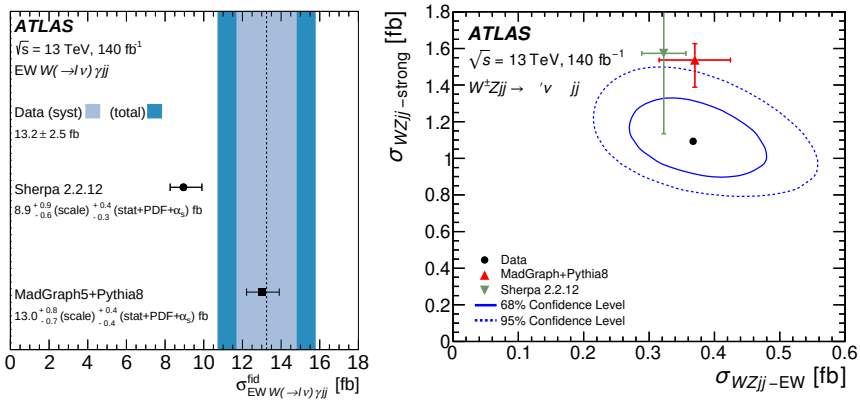

Fig. 3. Left: The measured electroweak (EW) $W\gamma jj$ fiducial cross section compared with the predictions of Sherpa and MadGraph5+PYTHIA 8. The central value of the measured fiducial cross section is represented by a dashed vertical line. The light shaded band represents the systematic uncertainty on the measured fiducial cross section, while the darker shaded band represents the total uncertainty [17]. Right: The measured electroweak ($\sigma_{WZjj-\mathrm{EW}}$) and strong ($\sigma_{WZjj-\mathrm{strong}}$) integrated cross sections compared with predictions from MadGraph+PYTHIA 8 (upward-pointing triangle) and Sherpa 2.2.12 (downward-pointing triangle). The full and dashed contours around the data points correspond to 68% and 95% confidence levels, respectively [18].

These rare processes provide valuable sensitivity to anomalous quartic gauge couplings. To probe potential deviations from the Standard Model, ATLAS uses an effective field theory framework to interpret measurements of multiboson production cross sections. The ATLAS Collaboration has set upper limits on the Wilson coefficients associated with different dimension-8 operators, both with and without unitarity-preserving techniques [17, 20]. Table 2 shows an example of limits on dimension-8 operators obtained without any unitarity-preserving techniques. Constraints on the Wilson coefficients for the T3 (f_{T3}/Λ^4) and T4 (f_{T4}/Λ^4) operators are the first constraints obtained using LHC data.

Table 2. Expected and observed limits on dimension-8 operators modifying the $WW\gamma\gamma$ coupling when fitting either the p_{T}^{jj} or p_{T}^{l} distribution of $W\gamma jj$ events produced via vector boson scattering [17].

Coefficients [TeV^{-4}]	Observable	Expected [TeV^{-4}]	Observed [TeV^{-4}]
f_{T0}/Λ^4	p_{T}^{jj}	$[-2.4, 2.4]$	$[-1.8, 1.8]$
f_{T1}/Λ^4	p_{T}^{jj}	$[-1.5, 1.6]$	$[-1.1, 1.2]$
f_{T2}/Λ^4	p_{T}^{jj}	$[-4.4, 4.7]$	$[-3.1, 3.5]$
f_{T3}/Λ^4	p_{T}^{jj}	$[-3.3, 3.5]$	$[-2.4, 2.6]$
f_{T4}/Λ^4	p_{T}^{jj}	$[-3.0, 3.0]$	$[-2.2, 2.2]$
f_{T5}/Λ^4	p_{T}^{jj}	$[-1.7, 1.7]$	$[-1.2, 1.3]$
f_{T6}/Λ^4	p_{T}^{jj}	$[-1.5, 1.5]$	$[-1.0, 1.1]$
f_{T7}/Λ^4	p_{T}^{jj}	$[-3.8, 3.9]$	$[-2.7, 2.8]$
f_{M0}/Λ^4	p_{T}^{l}	$[-28, 28]$	$[-24, 24]$
f_{M1}/Λ^4	p_{T}^{l}	$[-43, 44]$	$[-37, 38]$
f_{M2}/Λ^4	p_{T}^{l}	$[-10, 10]$	$[-8.6, 8.5]$
f_{M3}/Λ^4	p_{T}^{l}	$[-16, 16]$	$[-13, 14]$
f_{M4}/Λ^4	p_{T}^{l}	$[-18, 18]$	$[-15, 15]$
f_{M5}/Λ^4	p_{T}^{l}	$[-17, 14]$	$[-14, 12]$
f_{M7}/Λ^4	p_{T}^{l}	$[-78, 77]$	$[-66, 65]$

4. Summary

Recent ATLAS electroweak measurements explore both precision observables and rare processes with unprecedented detail. The W-boson mass and width measurements demonstrate the experiment's capacity for precise Standard Model tests. Studies of diboson polarization and quartic couplings offer avenues to uncover possible deviations from Standard Model expectations. As data accumulates and analysis techniques evolve, the potential for new discoveries remains strong.

REFERENCES

[1] ATLAS Collaboration (G. Aad *et al.*), *J. Instrum.* **3**, S08003 (2008).

[2] ATLAS Collaboration (G. Aad *et al.*), *Eur. Phys. J. C* **84**, 1309 (2024).

[3] CDF Collaboration (T. Aaltonen *et al.*), *Science* **376**, 170 (2022).

[4] ALEPH, DELPHI, L3, OPAL collaborations and LEP Electroweak Working Group (S. Schael *et al.*), *Phys. Rep.* **532**, 119 (2013).

[5] D0 Collaboration (V.M. Abazov *et al.*), *Phys. Rev. Lett.* **108**, 151804 (2012).

[6] ATLAS Collaboration (M. Aaboud *et al.*), *Phys. J. C* **78**, 110 (2018); *Erratum ibid.* **78**, 898 (2018).

[7] LHCb Collaboration (R. Aaij *et al.*), *J. High Energy Phys.* **2022**, 036 (2022).

[8] ATLAS Collaboration (G. Aad *et al.*), arXiv:2412.11644 [hep-ex], submitted to *Eur. Phys. J. C*.

[9] ATLAS Collaboration (G. Aad *et al.*), *Phys. Lett. B* **854**, 138725 (2024).

[10] ATLAS Collaboration (G. Aad *et al.*), *Phys. Lett. B* **855**, 138764 (2024).

[11] ATLAS Collaboration, https://atlas.web.cern.ch/Atlas/GROUPS/PHYSICS/CombinedSummaryPlots/SM/

[12] ATLAS Collaboration (G. Aad *et al.*), *Phys. Rev. Lett.* **133**, 161804 (2024).

[13] CDF Collaboration (T. Aaltonen *et al.*), *Phys. Rev. D* **85**, 032001 (2012).

[14] ATLAS Collaboration (G. Aad *et al.*), *Phys. Lett. B* **854**, 138705 (2024).

[15] ALEPH, DELPHI, L3, OPAL, SLD collaborations, LEP Electroweak Working Group, SLD Electroweak and Heavy Flavour Groups (S. Schael *et al.*), *Phys. Rep.* **427**, 257 (2006).

[16] ATLAS Collaboration (G. Aad *et al.*), *Phys. Rev. Lett.* **133**, 101802 (2024); *Erratum ibid.* **133**, 169901 (2024).

[17] ATLAS Collaboration (G. Aad *et al.*), *Eur. Phys. J. C* **84**, 1064 (2024).

[18] ATLAS Collaboration (G. Aad *et al.*), *J. High Energy Phys.* **2024**, 192 (2024).

[19] ATLAS Collaboration (G. Aad *et al.*), *Phys. Lett. B* **848**, 138400 (2024).

[20] ATLAS Collaboration (G. Aad *et al.*), *Phys. Lett. B* **866**, 139527 (2025).